

Backscatter-Assisted Wireless Powered Communication Networks Empowered by Intelligent Reflecting Surface

Parisa Ramezani, *Graduate Student Member, IEEE*, and Abbas Jamalipour, *Fellow, IEEE*

Abstract—Intelligent reflecting surface (IRS) has recently been emerged as an effective way for improving the performance of wireless networks by reconfiguring the propagation environment through a large number of passive reflecting elements. This game-changing technology is especially important for stepping into the Internet of Everything (IoE) era, where high performance is demanded with very limited available resources. In this paper, we study a backscatter-assisted wireless powered communication network (BS-WPCN), in which a number of energy-constrained users, powered by a power station (PS), transmit information to an access point (AP) via backscatter and active wireless information transfer, with their communication being aided by an IRS. Using a practical energy harvesting (EH) model which is able to capture the characteristics of realistic energy harvesters, we investigate the maximization of total network throughput. Specifically, IRS reflection coefficients, PS transmit and AP receive beamforming vectors, power and time allocation are designed through a two-stage algorithm, assuming minimum mean square error (MMSE) receiver at the AP. The effectiveness of the proposed algorithm is confirmed via extensive numerical simulations. We also show that our proposed scheme is readily applicable to practical IRS-aided networks with discrete phase shift values.

Index Terms—Wireless powered communication network, backscatter communication, intelligent reflecting surface, minimum mean square error.

I. INTRODUCTION

Wireless powered communication network (WPCN) is a network where devices are wirelessly powered by radio frequency (RF) signals transmitted by dedicated or ambient RF sources. Enabling devices to obtain their required energy in a self-sustainable manner, WPCN is regarded as an inevitable component of the much-anticipated Internet of Everything (IoT) [1]–[3]. Yet, like any other technology, WPCN has its own shortcomings. WPCN devices need sufficient time to harvest and accumulate their required energy before being able to take part in communication. This energy accumulation time can be long if the conditions are not favorable for harvesting energy. Longer energy harvesting (EH) time translates to shorter time being remained for information transmission (IT), which negatively impacts the network performance. As another important enabler for IoT, backscatter communication allows devices to transmit information to their intended receivers without needing to generate active RF signals. In backscatter transmission, devices modulate their information onto the

impinging RF signals and reflect them toward their intended receiver. Specifically, a portion of the incident signal power is used for powering the backscatter transmission, while the remaining part is reflected for information transfer. Integration of backscatter communication with WPCN is a promising way to alleviate the above-mentioned shortcoming of WPCNs as it lets devices perform IT without needing to wait for energy accumulation.

Backscatter communication is not the only technique which operates based on the reflection of wireless signals. Recently, a new technology has come on the scene, with the potential to remarkably enhance the performance of various wireless systems. This technology, referred to as intelligent reflecting surface (IRS), has lately been on the research spotlight due to its capability to modify the propagation environment. IRS is composed of a large number of low-cost passive reflecting elements which can be adaptively configured to impose phase and amplitude changes on the received signal and reflect it to the desired direction. The modification applied by IRS can compensate for poor channel conditions and allow devices to communicate even if there exists blockage between the transmitter and the receiver.

A. Related Work

The term WPCN was first introduced in [4], where the authors studied the uplink IT of a number of users to a hybrid access point (HAP) which also served the role of a downlink energy transmitter for the users. Since then, WPCN has gained considerable attention as an indispensable building block for the realization of the self-sustainable IoE. Extensive research has been done for extending WPCNs and improving their performance, among which we can name designing energy beamforming vectors [5], [6], adding full-duplex (FD) operation for simultaneous downlink energy and uplink information transfer [7], designing channel acquisition techniques for more accurate energy beamforming [8], enabling cooperation mechanisms [9]–[11], using power beacons (PBs) to enhance the efficiency of wireless energy transfer (WET) [12], and integrating this technology with relay-based communication networks [13]–[16]. Readers can refer to [1]–[3] for more details on the fundamentals of WPCN.

The integration of backscatter communication with WPCN has been proposed to support uninterrupted communication when there is not enough harvested energy to perform active wireless powered transmission. The low energy consumption

of backscatter communication make the instantaneous harvested energy sufficient for information transfer. Using the RF energy signals for both EH and backscatter transmission improves the performance of WPCNs and allows for more efficient utilization of available resources [17], [18]. References [19], [20] provide comprehensive surveys on backscatter communication and the benefits of integrating this technology with WPCN.

IRS has recently been applied to various wireless communication networks and demonstrated preeminent performance improvements. In [21], a single-user multiple-input single-output (MISO) communication system is considered, where an IRS assists in downlink communication between the access point (AP) and the user. The beamformer at the AP and the phase shifts at the IRS are jointly optimized for maximizing the spectral efficiency. Considering the practical limitations of IRS elements, [22] and [23] propose novel channel estimation techniques for IRS-assisted wireless networks. Capacity maximization problem for a point-to-point IRS-assisted multiple-input multiple-output (MIMO) system is investigated in [24]. In this work, the authors optimize the transmit covariance matrix as well as the IRS phase shifts, for narrowband and broadband MIMO systems. A multiuser MIMO system is considered in [25], where an IRS aids the uplink communication between a number of users and a base station (BS), while at the same time it delivers additional information by the on-off reflecting modulation. In [26], the communication between a source-destination pair is assumed to be assisted by both an IRS and an FD relay. IRS phase shifts as well as power allocation for the source and the FD relay are optimized to maximize the minimum achievable rate of the two hops. An IRS-assisted simultaneous wireless information and power transfer (SWIPT) system is proposed in [27] with an AP transmitting downlink energy and information to a set of EH receivers and information decoding receivers, respectively. Recently, a few works have studied the application of IRS to WPCNs [28], [29]. Reference [28] studies a two-user WPCN, where one of the users acts as a relay for the other. An IRS is employed for improving the performance of downlink energy transfer from the HAP to the users, uplink IT from users to the HAP, and the IT between the users. The authors optimize time and power allocation as well as the phase shift design at the IRS to maximize the common throughput of the two users. In [29], a WPCN with multiple users is considered, where a self-sustainable IRS empowers the energy and information transfer between the HAP and the users. Time-switching (TS) and power-splitting (PS) schemes are studied for EH at the IRS and the authors optimize the IRS phase shifts, time and power allocation, and TS/PS ratios. In all the above-mentioned works, IRS has been confirmed to bring significant performance improvements into existing wireless communication networks by fulfilling the long-lasting dream of modifying the wireless propagation environment. Reference [30] provides an overview of the IRS technology, compares it to other relevant technologies and reflects on some of the design challenges in IRS-assisted networks. The readers can also refer to [31], [32] for a more profound survey on IRS-assisted systems and directions for future research in this area.

B. Motivation

WPCN has been recognized as an indispensable component of IoE networks. Further, the introduction of backscatter assisted WPCNs (BS-WPCNs) has made it possible to reap the benefits of both backscatter communication and wireless powered communication technologies and utilize resources more efficiently. With the advancements of IRS technology, more performance improvements for BS-WPCNs can be foreseen. This is particularly important in scenarios where the channel conditions between the users and the AP is not favorable (due to e.g., long distance, blockage, etc.) and the direct transmission of users to the AP results in very low throughputs. IRS with its channel modification properties can be very useful in such cases by making additional links of high quality between the users and the AP.

To avoid mismatch between theoretical studies and real-life implementations, it is important to use simple and realistic models for the network elements. In light of this, the EH circuit of wireless powered devices need to be carefully modeled to capture the limitations of practical circuits, while being tractable and easy to follow. The conventional linear EH model used in most of the works on WPCN (e.g. [4]) is not valid due to disregarding the fundamental features of practical EH circuits. The well-known sigmoidal EH model [35], [36] which accounts for the practical EH characteristics has also tractability issues. Therefore, there is a compelling need for a simple and tractable way for modeling the behavior of EH circuits.

The above-mentioned points have motivated us to study the performance gains brought by employing IRS in BS-WPCNs, where a piece-wise linear EH model with three pieces is presented for modeling the relationship between received and harvested powers, which takes into consideration the two important characteristics of practical EH circuits, namely, sensitivity and saturation.

C. Contributions

In this paper, we consider a BS-WPCN, where the EH users are powered by WET from a power station (PS) and their information transfer to the AP is aided by an IRS. Our main contributions are summarized as follows:

- We propose an IRS-empowered BS-WPCN, where multiple users transmit information to an AP via backscatter and active information transfer. A PS is deployed to power the energy-constrained users and the IRS assists the information transfer of the users by adjusting the reflection coefficients of its elements. To the authors' best knowledge, this is the first work to study the integration of IRS with the hybrid of active wireless powered communication and passive backscatter communication.
- One of the most important design considerations in EH-enabled networks that is often overlooked is the non-linear input-output relationship of practical EH circuits. We propose to use a piece-wise linear EH model with three pieces at the users, which accounts for the sensitivity and saturation effects of practical energy harvesters. We verify the accuracy of this model by applying it to several

real measurements and comparing the real measured values with the ones estimated via this model.

- We formulate a sum-throughput maximization problem and study the optimization of IRS reflection coefficients (including both amplitude reflection and phase shift at each element), time and power allocation, transmit beamforming at the PS, and receive beamforming at the AP, under the practical average and peak power constraints at the PS as well as the energy causality constraint at the users. We propose a two-stage algorithm for solving the optimization problem, where the IRS reflection coefficients for empowering the users' backscatter communication are optimized in the first stage and the optimization of other variables is carried out in the second stage.
- We propose two different methods for optimizing the IRS reflection coefficients in the first stage based on classic alternating optimization (AO) and successive approximation (SA) techniques. For the second-stage optimization which involves optimizing the PS transmit beamforming, AP receive beamforming, time and power allocation, and the coefficients of the IRS when assisting users' active IT, we propose solutions based on the SA technique and the well-known semidefinite relaxation (SDR). Further, assuming minimum mean square error (MMSE) receiver at the AP, an efficient method is proposed based on the block coordinate descent (BCD) technique. As closed-form solutions are acquired in each iteration of the BCD procedure, the algorithm is guaranteed to converge to an optimal solution for AP receive beamforming and IRS reflection coefficients.
- We validate the efficiency of the proposed scheme by conducting extensive numerical simulations. We first evaluate the performance of the AO- and SA-based methods in the first stage of the algorithm and use the one with better throughput results for executing the simulations. We also validate the tightness of the rank-one approximation used for obtaining the beamforming vectors at the PS. We then compare the proposed algorithm with two benchmarks to show the remarkable improvements attained by introducing IRS into the BS-WPCN. We also show that the presented algorithm can be readily applied to the scenario with practical IRS settings, where only a limited number of phase shifts can be chosen for the IRS elements. We particularly show that a 2-bit resolution for the phase shift of IRS elements is sufficient for achieving the envisioned near-optimal performance.

D. Organization and Notations

Organization: We present the system model and formulate the throughput maximization problem in Section II. The two-stage algorithm for solving the formulated problem is elaborated in Sections III and IV. Numerical simulations for evaluating the performance of the proposed algorithms are presented in Section V, and Section VI concludes the paper and provides directions for future research.

Notations: Scalars are denoted by italic letters, vectors and matrices are denoted by bold-face lower-case and upper-case

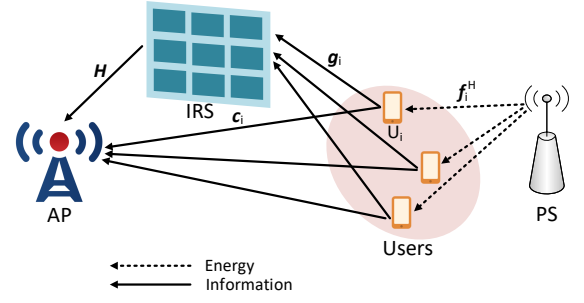


Fig. 1: An IRS-empowered BS-WPCN

letters, respectively. $(\cdot)^T$, $(\cdot)^H$, and $(\cdot)^{-1}$ denote transpose, Hermitian transpose, and matrix inversion operations, while $\text{Tr}(\cdot)$ and $\text{Rank}(\cdot)$ denote the matrix trace and rank, respectively. $\mathbb{C}^{a \times b}$ is the space of $a \times b$ complex-valued matrices. $\mathbb{E}[\cdot]$ stands for expectation and \mathbf{I}_M denotes the identity matrix of size M . $\text{Re}\{\cdot\}$, $|\cdot|$, $\arg(\cdot)$, and $\overline{(\cdot)}$ denote the real part, absolute value, angle, and conjugate of a complex number, respectively. $\|\cdot\|$ is the 2-norm of a vector and $[\cdot]_{i,j}$ indicates the element in the i th row and the j th column of a matrix. The distribution of a circularly symmetric complex Gaussian (CSCG) random vector is denoted by $\mathcal{CN}(\mu, \Sigma)$ with μ being the mean vector and Σ representing the covariance matrix. \sim stands for "distributed as" and \cup is the union operator.

II. SYSTEM MODEL AND PROBLEM FORMULATION

We consider a multi-user BS-WPCN, as shown in Fig. 1, where the users are wirelessly powered by a PS to transmit their information to an AP. In addition to collecting energy from the PS transmissions, the users also backscatter the received signals from the PS to transmit information to the AP in a time division multiple access (TDMA) manner. The harvested energy will then be used by the users to actively transmit information signals to the AP via space division multiple access (SDMA). The backscatter and active IT of the users are aided by IRS elements which induce amplitude and phase changes to the signals transmitted by the users such that the signals from different paths are constructively added at the AP.

The PS and AP are equipped with M_P and M_A antennas, respectively, while each user has one single antenna. Also, the IRS consists of N reflecting elements. We denote by $\mathcal{K} = \{1, \dots, K\}$ and $\mathcal{N} = \{1, \dots, N\}$ the set of all users and IRS reflecting elements, respectively. $\mathbf{F}^H \in \mathbb{C}^{K \times M_P}$, $\mathbf{G} \in \mathbb{C}^{N \times K}$, $\mathbf{C} \in \mathbb{C}^{M_A \times K}$, and $\mathbf{H} \in \mathbb{C}^{M_A \times N}$ respectively represent the PS-users, users-IRS, users-AP, and IRS-AP channel matrices. In this work, CSI is obtained based on the techniques proposed in [8], [22], [23].

In this section, we present the system model including the EH model and the communication model, and formulate the sum-throughput maximization problem. Specifically, we provide a brief overview of practical EH circuits and explain the inefficacy of the conventional linear EH model in modeling the behavior of EH circuits. We then introduce the EH model used in this work and provide illustrations to confirm its accuracy for EH modeling. Then, the communication model is

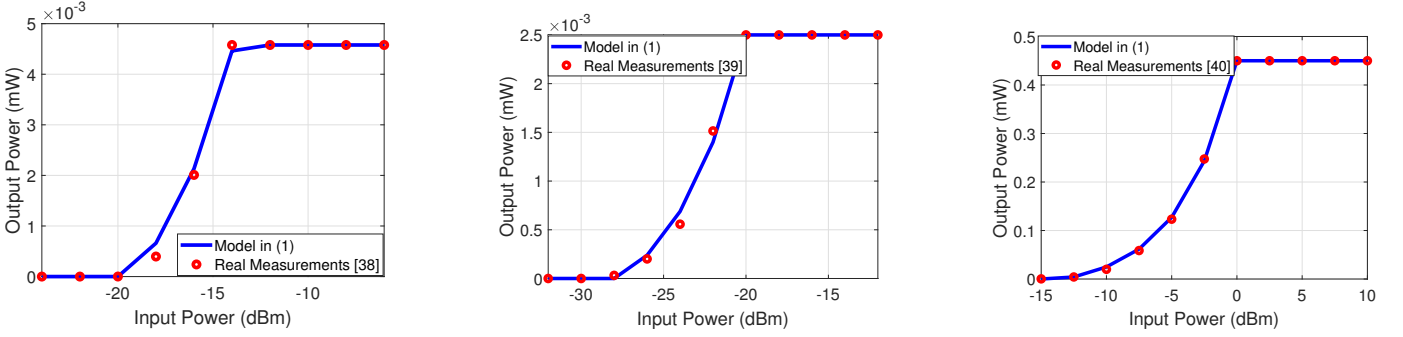


Fig. 2: Comparison between the model in (1) and real measurements in [38]–[40]

presented followed by the formulation of the sum-throughput maximization problem, which aims to optimize the IRS reflection coefficients for backscatter and active information transfer as well as the transmit beamforming vectors of the PS, receive beamforming vectors of the AP, power allocation of the users and time allocation for EH and IT.

A. EH Model

Most EH circuits use diode-based rectifiers to convert the received RF power into dc power. The efficiency of diode-based energy harvesters highly depends on the level of the received power. Specifically, when the received power is below the sensitivity of the energy harvester, the output power is zero because low input powers cannot turn on the diode. More importantly, when the received power exceeds some specific levels, the energy conversion efficiency is greatly degraded [33]; however, the output dc power remains constant and becomes saturated [34]. This saturation point depends on the reverse breakdown voltage. As the reverse breakdown voltage increases, the maximum achievable output power also increases; however, saturation is unavoidable and there always exists a maximum level for the output power. Taking into account the saturation effect is pivotal when studying networks with EH-enabled devices. Without considering this effect, the theoretical optimal design fails to perform properly in practice. Therefore, the conventional linear EH model, in which the output power linearly increases with the received power, cannot be relied on for studying the behavior of EH circuits. The sigmoidal EH model has recently been used by many researchers for designing resource allocation schemes in EH networks [35], [36]. However, this model cannot be easily implemented in convex optimization toolboxes such as CVX [37] without further approximations and transformations, especially when the received power varies over the harvesting period and the harvested power becomes a sum-of-ratios expression. Another EH model has been used in the literature which models the input-output power relationship of an energy harvester with a piece-wise linear function with two pieces, where the output power linearly increases with the input power up to the saturation point, beyond which the output power remains constant [16], [18]. This model is more tractable than the sigmoidal model, however, it does not account for the sensitivity of EH circuits.

In this paper, we use a piece-wise linear EH model with three pieces, where both sensitivity and saturation effects are taken into consideration. The harvested power in this model is given by

$$p_h = \min(\max(0, \eta p_r - \xi), p_{\text{sat}}), \quad (1)$$

where p_h and p_r are the harvested power and the received power, respectively, p_{sat} is the saturation power and $\frac{\xi}{\eta}$ is the turn-on power.

In Fig. 2, we have plotted the curve fitting results for the piece-wise linear EH model in (1) using real measurements from [38]–[40]. The figure shows the good match between the model in (1) and real data, which confirms that this model is accurate enough for modeling the behavior of realistic EH circuits.

B. Communication Model

The transmission block for the system is depicted in Fig. 3, which begins with PS acting as both energy and signal source for the users, transmitting unmodulated RF signals in the downlink. Unlike the conventional WPCN, where the transmitted signals of the PS are merely used as a source of energy, the users of BS-WPCN make a more efficient use of these signals. In addition to harvesting their required energy, the users also modulate their information onto the signals and transmit them towards the AP using the backscattering technique. The backscatter transmission of the users is performed in a TDMA manner such that each user gets a dedicated time slot for performing backscatter transmission to the AP. Specifically, time slot i of duration τ_i is allocated to backscatter transmission of the i th user, denoted as U_i , while other users harvest energy from the signal transmitted by the PS. During τ_{K+1} ¹, all users simultaneously transmit to the AP, using their previously harvested energy. Both backscatter and active IT of the users are aided by IRS elements which apply phase and amplitude adjustments to the incident signals and reflect them to the AP. We assume perfect synchronization among network elements. The reflection coefficient adjustment of IRS elements is performed by an IRS controller [21], [24], [25].

During τ_i , $\forall i \in \mathcal{K}$, the PS transmits $\mathbf{w}_i \hat{s}_i$ in the downlink, where \mathbf{w}_i is the beamforming vector of the PS and \hat{s}_i is an

¹Henceforth, time slots are represented by their duration, i.e., by τ_i we mean time slot i .

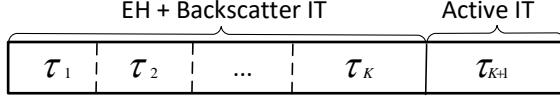


Fig. 3: Transmission block structure for the IRS-empowered BS-WPCN

unmodulated signal with unit power. The received signal at U_i is given by $\mathbf{f}_i^H \mathbf{w}_i \hat{s}_i$, where \mathbf{f}_i^H is the i -th row of \mathbf{F}^H . U_i uses a portion of the received signal power for powering its circuit operations during backscatter transmission and reflects the remaining portion for transmitting information to the AP. Denote by β_i the backscatter coefficient of U_i . The transmitted signal of U_i during τ_i is given by $x_{1,i} = \sqrt{\beta_i} \mathbf{f}_i^H \mathbf{w}_i s_{1,i} \hat{s}_i$, where $s_{1,i}$ is the information-bearing signal of U_i with $\mathbb{E}\{|s_{1,i}|^2\} = 1$. Each IRS element applies amplitude and phase changes to the received signal and reflects it to the AP. The received signal at the AP during τ_i , $\forall i \in \mathcal{K}$ is obtained as

$$\mathbf{y}_{1,i} = (\mathbf{H}\mathbf{\Theta}_i \mathbf{g}_i + \mathbf{c}_i)x_{1,i} + \mathbf{n}, \quad (2)$$

where $\mathbf{n} \sim \mathcal{CN}(0, \sigma^2 \mathbf{I}_{M_A})$ is the additive white Gaussian noise (AWGN) at the AP, \mathbf{g}_i and \mathbf{c}_i are the i -th columns of \mathbf{G} and \mathbf{C} , respectively, and $\mathbf{\Theta}_i$ is the reflection matrix of the IRS during τ_i given by

$$\mathbf{\Theta}_i = \begin{bmatrix} \alpha_{1,i} e^{j\theta_{1,i}} & & \\ & \ddots & \\ & & \alpha_{N,i} e^{j\theta_{N,i}} \end{bmatrix}$$

with $\alpha_{n,i}$ and $\theta_{n,i}$ respectively representing the amplitude reflection coefficient and phase shift applied by the n -th element of IRS during τ_i .

From (2) and after maximum ratio combining (MRC) at the AP, the signal-to-noise ratio (SNR) of U_i is given by

$$\gamma_{1,i} = \frac{\beta_i |\mathbf{f}_i^H \mathbf{w}_i|^2 \|\mathbf{h}_i(\mathbf{\Theta}_i)\|^2}{\sigma^2}, \quad (3)$$

with $\mathbf{h}_i(\mathbf{\Theta}_i) = \mathbf{H}\mathbf{\Theta}_i \mathbf{g}_i + \mathbf{c}_i$ being the effective channel between AP and U_i during τ_i . The achievable throughput of U_i during τ_i is obtained as

$$R_{1,i} = \tau_i \log(1 + \gamma_{1,i}) = \tau_i \log\left(1 + \frac{\beta_i |\mathbf{f}_i^H \mathbf{w}_i|^2 \|\mathbf{h}_i(\mathbf{\Theta}_i)\|^2}{\sigma^2}\right). \quad (4)$$

While U_i backscatters the transmitted signal of PS for information transfer, other users harvest energy from this signal. The harvested energy of U_j $j \neq i$ during τ_i is given by

$$e_{h,j,i} = \tau_i p_{h,j,i}, \quad (5)$$

where $p_{h,j,i}$ is the harvested power of U_j during τ_i and is given by³

$$p_{h,j,i} = \min(\max(0, \eta |\mathbf{f}_j^H \mathbf{w}_i|^2 - \xi), p_{\text{sat}}). \quad (6)$$

The users utilize their harvested energy for actively transmitting information to the AP. Denote by $s_{2,i}$ the information signal of U_i in τ_{K+1} and by p_i the transmit power of U_i .

The transmitted signal of U_i during τ_{K+1} is then given by $x_{2,i} = \sqrt{p_i} s_{2,i}$. The transmitted signal of the users is again reflected by the IRS which applies the reflection matrix $\mathbf{\Theta}_{K+1}$ to the signal and transmits it to the AP. The received signal at the AP is given by

$$\mathbf{y}_2 = \sum_{i=1}^K \mathbf{h}_i(\mathbf{\Theta}_{K+1}) x_{2,i} + \mathbf{n}, \quad (7)$$

where $\mathbf{h}_i(\mathbf{\Theta}_{K+1}) = \mathbf{H}\mathbf{\Theta}_{K+1} \mathbf{g}_i + \mathbf{c}_i$ and $\mathbf{\Theta}_{K+1}$ is defined similar to $\mathbf{\Theta}_i$ with $\alpha_{n,i}$ and $\theta_{n,i}$ being replaced by $\alpha_{n,K+1}$ and $\theta_{n,K+1}$, $\forall n \in \mathcal{N}$.

The AP applies the receive beamforming vector \mathbf{a}_i for decoding the signal of U_i . The SINR and achievable throughput of U_i for active IT are respectively obtained as

$$\gamma_{2,i} = \frac{p_i |\mathbf{a}_i^H \mathbf{h}_i(\mathbf{\Theta}_{K+1})|^2}{\sum_{j \neq i} p_j |\mathbf{a}_i^H \mathbf{h}_j(\mathbf{\Theta}_{K+1})|^2 + \|\mathbf{a}_i^H\|^2 \sigma^2}, \quad (8)$$

$$R_{2,i} = \tau_{K+1} \log(1 + \gamma_{2,i}) \\ = \tau_{K+1} \log\left(1 + \frac{p_i |\mathbf{a}_i^H \mathbf{h}_i(\mathbf{\Theta}_{K+1})|^2}{\sum_{j \neq i} p_j |\mathbf{a}_i^H \mathbf{h}_j(\mathbf{\Theta}_{K+1})|^2 + \|\mathbf{a}_i^H\|^2 \sigma^2}\right). \quad (9)$$

C. Problem Formulation

We aim to maximize the total throughput of the network by optimizing IRS reflection coefficients in all time slots, the transmit beamforming at the PS, the receive beamforming at the AP, the power allocation of the users for active IT, and the time allocation of the network. The sum-throughput maximization problem is thus formulated as

$$\max_{\{\mathbf{\Theta}_i\}_{i=1}^K, \mathbf{\Theta}_{K+1}, \{\mathbf{w}_i\}_{i=1}^K, \{\mathbf{a}_i\}_{i=1}^K, \mathbf{p}, \boldsymbol{\tau}} \sum_{i=1}^K R_{1,i} + R_{2,i} \quad (10)$$

$$\text{s.t.} \quad \sum_{i=1}^K \tau_i \text{Tr}(\mathbf{w}_i \mathbf{w}_i^H) \leq p_{\text{avg}}, \quad (10.a)$$

$$\text{Tr}(\mathbf{w}_i \mathbf{w}_i^H) \leq p_{\text{peak}}, \quad \forall i \in \mathcal{K}, \quad (10.b)$$

$$(p_i + p_{c,i}) \tau_{K+1} \leq \sum_{j \neq i} e_{h,i,j}, \quad \forall i \in \mathcal{K}, \quad (10.c)$$

$$\sum_{i=1}^K \tau_i + \tau_{K+1} \leq 1, \quad (10.d)$$

$$p_i \geq 0, \forall i \in \mathcal{K}, \quad \tau_i \geq 0, \quad \forall i \in \mathcal{K} \cup \{K+1\}, \quad (10.e)$$

$$0 \leq \alpha_{n,i} \leq 1, \quad -\pi < \theta_{n,i} \leq \pi \\ \forall n \in \mathcal{N}, \quad i \in \mathcal{K} \cup \{K+1\}, \quad (10.f)$$

where $\mathbf{p} = [p_1, \dots, p_K]$, and $\boldsymbol{\tau} = [\tau_1, \dots, \tau_{K+1}]$. Constraints (10.a) and (10.b) account for the average power constraint and peak power constraint at the PS, respectively. Constraint (10.c) is the energy causality constraint at the users with $p_{c,i}$ denoting the circuit power consumption at U_i for active information transfer. Constraint (10.d) is the total time constraint assuming a normalized transmission block. Constraints (10.e) and (10.f) define the acceptable range for the optimization variables. The

²We ignore noise at the users because no signal processing is performed.

³Without loss of generality, we assume that the EH circuits of all users are similar such that the same EH parameters are used for all users.

problem in (10) is non-convex and challenging to solve. In the following, we propose a two-stage scheme, where the IRS reflection coefficients for backscatter transmission are optimized in the first stage and the optimization of other variables is performed in the second stage. Note that the schemes proposed in this paper can also be used to solve the weighted sum-throughput maximization problem, where the weights can be arbitrarily set to indicate user priorities and to control user fairness.

III. IRS REFLECTION FOR BACKSCATTER COMMUNICATION

The IRS reflection optimization problem for users' backscatter transmission is given by

$$\begin{aligned} \max_{\{\Theta_i\}_{i=1}^K} \quad & \sum_{i=1}^K \tau_i \log(1 + \hat{\beta}_i \|\mathbf{h}_i(\Theta_i)\|^2) \\ \text{s.t.} \quad & 0 \leq \alpha_{n,i} \leq 1, \quad -\pi < \theta_{n,i} \leq \pi, \quad \forall n \in \mathcal{N}, i \in \mathcal{K}, \end{aligned} \quad (11)$$

where $\hat{\beta}_i = \frac{\beta_i \|\mathbf{f}_i^H \mathbf{w}_i\|^2}{\sigma^2}$.

We can split the problem in (11) into K separate sub-problems, each dealing with the optimization of the IRS reflection coefficients in one of the time slots. Specifically, the i -th sub-problem will be

$$\begin{aligned} \max_{\Theta_i} \quad & \|\mathbf{h}_i(\Theta_i)\|^2 = \|\mathbf{H}\Theta_i \mathbf{g}_i + \mathbf{c}_i\|^2 \\ \text{s.t.} \quad & 0 \leq \alpha_{n,i} \leq 1, \quad -\pi < \theta_{n,i} \leq \pi, \quad \forall n \in \mathcal{N}. \end{aligned} \quad (12)$$

Defining $\mathbf{V}_i = \mathbf{H} \text{diag}(\mathbf{g}_i)$ and $\mathbf{u}_i = [u_{1,i}, \dots, u_{N,i}]^T$ with $u_{n,i} = \alpha_{n,i} \exp(j\theta_{n,i})$, $\forall n \in \mathcal{N}$, we have

$$\begin{aligned} \|\mathbf{H}\Theta_i \mathbf{g}_i + \mathbf{c}_i\|^2 &= (\mathbf{V}_i \mathbf{u}_i + \mathbf{c}_i)^H (\mathbf{V}_i \mathbf{u}_i + \mathbf{c}_i) \\ &= \mathbf{u}_i^H \mathbf{V}_i^H \mathbf{V}_i \mathbf{u}_i + 2\text{Re}\{\mathbf{u}_i^H \mathbf{V}_i^H \mathbf{c}_i\} + \|\mathbf{c}_i\|^2, \end{aligned} \quad (13)$$

and problem (12) can be re-written as

$$\begin{aligned} \max_{\mathbf{u}_i} \quad & \mathbf{u}_i^H \mathbf{V}_i^H \mathbf{V}_i \mathbf{u}_i + 2\text{Re}\{\mathbf{u}_i^H \mathbf{V}_i^H \mathbf{c}_i\} + \|\mathbf{c}_i\|^2 \\ \text{s.t.} \quad & |u_{n,i}| \leq 1, \quad \forall n \in \mathcal{N}. \end{aligned} \quad (14)$$

Problem (14) is a non-convex optimization problem because of the quadratic term $\mathbf{u}_i^H \mathbf{V}_i^H \mathbf{V}_i \mathbf{u}_i$ in the objective function. In the following, we propose two methods for solving problem (14). In the first method, we alternately optimize the reflection coefficient of one IRS element having other reflection coefficients fixed, in an iterative manner. The second method is based on the SA technique, where a lower-bound of the objective function is maximized iteratively until convergence is achieved.

A. AO-Based Design

Expanding the first two terms of the objective function in (14), we have

$$\begin{aligned} \mathbf{u}_i^H \mathbf{V}_i^H \mathbf{V}_i \mathbf{u}_i + 2\text{Re}\{\mathbf{u}_i^H \mathbf{V}_i^H \mathbf{c}_i\} &= \sum_{n=1}^N \left(|u_{n,i}|^2 \sum_{m=1}^{M_A} \|\mathbf{V}_i\|_{m,n}^2 + \right. \\ & \left. 2\text{Re}\{u_{n,i} (\sum_{q=n+1}^N \bar{u}_{q,i} (\sum_{m=1}^{M_A} [\mathbf{V}_i]_{m,n} [\mathbf{V}_i^H]_{q,m}) + \sum_{m=1}^{M_A} \bar{c}_{m,i} [\mathbf{V}_i]_{m,n})\} \right), \end{aligned} \quad (15)$$

where $c_{m,i}$ is the m -th element of \mathbf{c}_i .

The objective is to alternately optimize the reflection coefficients. The optimization problem for the n -th ($\forall n \in \mathcal{N}$) reflection coefficient in the i -th ($\forall i \in \mathcal{K}$) time slot is thus formulated as

$$\begin{aligned} \max_{u_{n,i}} \quad & t_{n,i} |u_{n,i}|^2 + 2\text{Re}\{z_{n,i} u_{n,i}\} \\ \text{s.t.} \quad & |u_{n,i}| \leq 1, \end{aligned} \quad (16)$$

where

$$\begin{aligned} t_{n,i} &= \sum_{m=1}^{M_A} \|\mathbf{V}_i\|_{m,n}^2 \\ z_{n,i} &= \sum_{q=1}^N \bar{u}_{q,i} (\sum_{m=1}^{M_A} [\mathbf{V}_i]_{m,n} [\mathbf{V}_i^H]_{q,m}) + \sum_{m=1}^{M_A} \bar{c}_{m,i} [\mathbf{V}_i]_{m,n}, \end{aligned}$$

and the terms independent of $u_{n,i}$ have been discarded. The optimal solution to (16) is readily obtained as

$$u_{n,i} = e^{-j\arg(z_{n,i})} \quad (17)$$

Algorithm 1 describes the above alternating procedure for optimizing the IRS reflection coefficients.

Algorithm 1: AO-Based Optimization of IRS Reflection Coefficients for Backscatter IT

```

Set  $u_{n,i}^{(0)} = 1, \forall n \in \mathcal{N}, i \in \mathcal{K}$ ;
for  $i = 1 : K$  do
     $\Delta = 1, l = 0$ ;
    while  $\Delta > \epsilon$  do
         $l = l + 1$ ;
        for  $n = 1 : N$  do
            Given  $u_{n',i}^{(l)}$  for  $n' = 1, \dots, n-1$  and  $u_{n'}^{(l-1)}$  for
             $n' = n+1, \dots, N$ , calculate  $z_{n,i}$ ;
            Find  $u_{n,i}^{(l)}$  from (17);
        end
         $\Delta = \|\mathbf{u}_i^{(l)} - \mathbf{u}_i^{(l-1)}\|$ ;
    end
    Set  $\alpha_{n,i}^* = |u_{n,i}^{(l)}|$  and  $\theta_{n,i}^* = \arg(u_{n,i}^{(l)})$ ,  $\forall n \in \mathcal{N}$ ;

```

Remark 1. Although the optimization of $u_{n,i}$ in (16) ensures that the power of the combined signal from the direct path and the n -th reflected path is improved, it does not necessarily mean that the power of the collective signal received at the AP is also increased. In other words, the separate optimization of IRS reflection coefficients may fail to result in coherent combination of the individually reflected signals at the AP. Therefore, the improvement of throughput over iterations is not guaranteed and the algorithm may converge to a sub-optimal solution. In what follows, we propose another method for finding the optimal reflection coefficients of IRS elements, based on the SA technique, with guaranteed throughput improvement after each update.

B. SA-Based Design

As mentioned earlier in this section, the non-convexity of problem (14) is due to the objective function being quadratic, which is convex in \mathbf{u}_i . At any feasible point $\mathbf{u}_i^{(0)}$, the term

$\mathbf{u}_i^H \mathbf{V}_i^H \mathbf{V}_i \mathbf{u}_i$ is lower-bounded by its first-order Taylor expansion as $2\text{Re}\{\mathbf{u}_i^H \mathbf{V}_i^H \mathbf{V}_i \mathbf{u}_i^{(0)}\} - \mathbf{u}_i^{(0)H} \mathbf{V}_i^H \mathbf{V}_i \mathbf{u}_i^{(0)}$. We can therefore apply the SA technique and iteratively maximize the lower-bound of the objective function in (14) until convergence. In iteration l , we will have the following optimization problem:

$$\begin{aligned} \max_{\mathbf{u}_i} & 2\text{Re}\{\mathbf{u}_i^H (\mathbf{V}_i^H \mathbf{V}_i \mathbf{u}_i^{(l-1)} + \mathbf{V}_i^H \mathbf{c}_i)\} + C_i^{(l-1)} \\ \text{s.t.} & (14.a), \end{aligned} \quad (18)$$

where $\mathbf{u}_i^{(l-1)}$ is the optimized \mathbf{u}_i in the $(l-1)$ -th iteration and $C_i^{(l-1)} = \|\mathbf{c}_i\|^2 - \mathbf{u}_i^{(l-1)H} \mathbf{V}_i^H \mathbf{V}_i \mathbf{u}_i^{(l-1)}$. Problem (18) is equivalent to

$$\begin{aligned} \max_{\mathbf{u}_i} & \text{Re}\left\{\sum_{n=1}^N \bar{u}_{n,i} \tilde{v}_{n,i}\right\} \\ \text{s.t.} & (14.a), \end{aligned} \quad (19)$$

where $\tilde{v}_{n,i}$ is the n -th element of $\tilde{\mathbf{v}}_i = \mathbf{V}_i^H \mathbf{V}_i \mathbf{u}_i^{(l-1)} + \mathbf{V}_i^H \mathbf{c}_i$. It is straightforward to see that the optimal solution to problem (19) is given by

$$u_{n,i} = e^{j\arg(\tilde{v}_{n,i})}, \quad \forall n \in \mathcal{N}. \quad (20)$$

The steps for optimizing the IRS reflection coefficients using the SA-based method is given in Algorithm 2.

Algorithm 2: SA-Based Optimization of IRS Reflection Coefficients for Backscatter IT

```

Set  $\mathbf{u}_{n,i}^{(0)} = 1, \forall n \in \mathcal{N}, i \in \mathcal{K}$ ;
for  $i=1:K$  do
     $\Delta = 1, l = 0$ ;
    while  $\Delta > \epsilon$  do
         $l = l + 1$ ;
        Calculate  $\tilde{\mathbf{V}}_i = \mathbf{V}_i^H \mathbf{V}_i \mathbf{u}_i^{(l-1)} + \mathbf{V}_i^H \mathbf{c}_i$ ;
        Find  $u_{n,i}^{(l)}, \forall n \in \mathcal{N}$  from (20);
         $\Delta = \|\mathbf{u}_i^{(l)} - \mathbf{u}_i^{(l-1)}\|$ ;
    Set  $\alpha_{n,i}^* = |u_{n,i}^{(l)}|$  and  $\theta_{n,i}^* = \arg(u_{n,i}^{(l)}), \forall n \in \mathcal{N}$ .

```

The objective function is guaranteed to improve after each iteration with Algorithm 2. Specifically, setting $\mathcal{F}(\mathbf{u}_i) = \mathbf{u}_i^H \mathbf{V}_i^H \mathbf{V}_i \mathbf{u}_i + 2\text{Re}\{\mathbf{u}_i^H \mathbf{V}_i^H \mathbf{c}_i\} + \|\mathbf{c}_i\|^2$, we have

$$\begin{aligned} \mathcal{F}(\mathbf{u}_i^{(l)}) & \stackrel{(\varpi_1)}{\geq} 2\text{Re}\{\mathbf{u}_i^{(l)H} (\mathbf{V}_i^H \mathbf{V}_i \mathbf{u}_i^{(l-1)} + \mathbf{V}_i^H \mathbf{c}_i)\} + C_i^{(l-1)} \\ & \stackrel{(\varpi_2)}{\geq} 2\text{Re}\{\mathbf{u}_i^{(l-1)H} (\mathbf{V}_i^H \mathbf{V}_i \mathbf{u}_i^{(l-1)} + \mathbf{V}_i^H \mathbf{c}_i)\} + C_i^{(l-1)} = \mathcal{F}(\mathbf{u}_i^{(l-1)}) \\ & \stackrel{(\varpi_3)}{\geq} 2\text{Re}\{\mathbf{u}_i^{(l-1)H} (\mathbf{V}_i^H \mathbf{V}_i \mathbf{u}_i^{(l-2)} + \mathbf{V}_i^H \mathbf{c}_i)\} + C_i^{(l-2)}, \quad \forall l, \end{aligned} \quad (21)$$

where (ϖ_1) and (ϖ_3) hold because $\mathcal{F}(\mathbf{u}_i)$ is lower-bounded by its first-order Taylor expansion, and (ϖ_2) is due to the fact that $\mathbf{u}_i^{(l)}$ is the optimal solution to (18) in the l -th iteration. Therefore, both the objective function in (14) and its lower-bound in (18) increase after each iteration.

IV. RESOURCE ALLOCATION, BEAMFORMING, AND IRS REFLECTION FOR ACTIVE COMMUNICATION

In order to find the near-optimal design for the remaining optimization variables, the AO technique is used by dividing the variables into groups and alternately optimizing them in an iterative manner. The details will be elaborated in the following subsections.

A. Design of Resource Allocation and Transmit Beamforming

We first investigate the optimization of resource allocation including power allocation at the users and time allocation for EH, backscatter IT, and active IT, as well as the transmit beamforming vectors of the PS. We have the following optimization problem:

$$\begin{aligned} \max_{\mathbf{p}, \tau, \{\mathbf{w}\}_{i=1}^K} & \sum_{i=1}^K \left(\tau_i \log\left(1 + \frac{\beta_i \|\mathbf{h}_i(\Theta_i)\|^2 |\mathbf{f}_i^H \mathbf{w}_i|^2}{\sigma^2}\right) \right. \\ & \left. + \tau_{K+1} \log\left(1 + \frac{p_i |\mathbf{a}_i^H \mathbf{h}_i(\Theta_{K+1})|^2}{\sum_{j \neq i} p_j |\mathbf{a}_i^H \mathbf{h}_j(\Theta_{K+1})|^2 + \|\mathbf{a}_i^H\|^2 \sigma^2}\right) \right) \\ \text{s.t.} & (10.a) - (10.e). \end{aligned} \quad (22)$$

The above problem is not a convex optimization problem because the objective function is not concave and the variables are coupled in the objective function and the constraints. We define $\tilde{\mathbf{W}}_i = \tau_i \mathbf{w}_i \mathbf{w}_i^H$, $e_i = \tau_{K+1} p_i$ and introduce auxiliary matrix Φ . Problem (22) is re-written as

$$\begin{aligned} \max_{\mathbf{e}, \tau, \{\tilde{\mathbf{W}}_i\}_{i=1}^K, \Phi} & \sum_{i=1}^K \left(\tau_i \log\left(1 + \tilde{\beta}_i \frac{\text{Tr}(\tilde{\mathbf{F}}_i \tilde{\mathbf{W}}_i)}{\tau_i}\right) \right. \\ & \left. + \tau_{K+1} \log\left(1 + \frac{\tilde{a}_{i,i} \frac{e_i}{\tau_{K+1}}}{\sum_{j \neq i} \tilde{a}_{i,j} \frac{e_j}{\tau_{K+1}} + \tilde{c}_i}\right) \right) \end{aligned} \quad (23)$$

$$\text{s.t.} \quad \sum_{i=1}^K \text{Tr}(\tilde{\mathbf{W}}_i) \leq p_{\text{avg}} \quad (23.a)$$

$$\text{Tr}(\tilde{\mathbf{W}}_i) \leq \tau_i p_{\text{peak}}, \quad \forall i \in \mathcal{K} \quad (23.b)$$

$$e_i + p_{c,i} \tau_{K+1} \leq \sum_{j \neq i} \min([\Phi]_{i,j}, \tau_j p_{\text{sat}}), \quad \forall i \in \mathcal{K} \quad (23.c)$$

$$\eta \text{Tr}(\tilde{\mathbf{F}}_i \tilde{\mathbf{W}}_j) \leq [\Phi]_{i,j} + \xi \tau_j, \quad \forall i, j \in \mathcal{K}, j \neq i, \quad (23.d)$$

$$\sum_{i=1}^K \tau_i + \tau_{K+1} \leq 1, \quad (23.e)$$

$$[\Phi]_{i,j} \geq 0, \quad \forall i, j \in \mathcal{K} \quad (23.f)$$

$$e_i \geq 0, \quad \forall i \in \mathcal{K}, \quad \tau_i \geq 0, \quad \forall i \in \mathcal{K} \cup \{K+1\}, \quad (23.g)$$

$$\tilde{\mathbf{W}}_i \geq 0, \quad \forall i \in \mathcal{K}, \quad (23.h)$$

$$\text{Rank}(\tilde{\mathbf{W}}_i) = 1, \quad \forall i \in \mathcal{K}, \quad (23.i)$$

where $\mathbf{e} = [e_1, \dots, e_K]$, $\tilde{\mathbf{F}}_i = \mathbf{f}_i \mathbf{f}_i^H$, $\tilde{\beta}_i = \frac{\beta_i \|\mathbf{h}_i(\Theta_i)\|^2}{\sigma^2}$, $\tilde{a}_{i,j} = |\mathbf{a}_i^H \mathbf{h}_j(\Theta_{K+1})|^2$, and $\tilde{c}_i = \|\mathbf{a}_i^H\|^2 \sigma^2$. Problem (23) is still non-convex because the second term of the objective

function is not concave and also the rank-one constraint in (23.i) is not convex. To deal with the non-concavity in the objective function, we write the second term of (23) as a sum of concave and convex functions and apply the SA technique to iteratively maximize a lower bound of the objective function. Specifically, we have

$$\begin{aligned} & \tau_{K+1} \log \left(1 + \frac{\tilde{a}_{i,i} \frac{e_i}{\tau_i}}{\sum_{j \neq i} \tilde{a}_{i,j} \frac{e_j}{\tau_{K+1}} + \tilde{c}_i} \right) = \\ & \tau_{K+1} \log \left(\sum_{j=1}^K \tilde{a}_{i,j} \frac{e_j}{\tau_{K+1}} + \tilde{c}_i \right) - \tau_{K+1} \log \left(\sum_{\substack{j=1 \\ j \neq i}}^K \tilde{a}_{i,j} \frac{e_j}{\tau_{K+1}} + \tilde{c}_i \right). \end{aligned} \quad (24)$$

In (24), $\tau_{K+1} \log \left(\sum_{j=1}^K \tilde{a}_{i,j} (e_j / \tau_{K+1}) + \tilde{c}_i \right)$ is a concave function since it is obtained by applying the perspective operation to the concave function $\log \left(\sum_{j=1}^K \tilde{a}_{i,j} e_j + \tilde{c}_i \right)$ and the perspective operation preserves concavity. On the other hand, $-\tau_{K+1} \log \left(\sum_{j \neq i} \tilde{a}_{i,j} (e_j / \tau_{K+1}) + \tilde{c}_i \right)$ is a jointly convex function of τ_{K+1} and \mathbf{e} , which motivates us to use the SA technique for solving (23). Based on the first-order Taylor series expansion, this convex function can be approximated by its lower bound as

$$\begin{aligned} & -\tau_{K+1} \log \left(\sum_{j \neq i} \tilde{a}_{i,j} \frac{e_j}{\tau_{K+1}} + \tilde{c}_i \right) \approx -\tau_{K+1}^{(0)} \log \left(\sum_{j \neq i} \tilde{a}_{i,j} \frac{e_j^{(0)}}{\tau_{K+1}^{(0)}} + \tilde{c}_i \right) \\ & + \left(\frac{\sum_{j \neq i} \tilde{a}_{i,j} \frac{e_j^{(0)}}{\tau_{K+1}^{(0)}}}{\sum_{j \neq i} \tilde{a}_{i,j} \frac{e_j^{(0)}}{\tau_{K+1}^{(0)}} + \tilde{c}_i} - \log \left(\sum_{j \neq i} \tilde{a}_{i,j} \frac{e_j^{(0)}}{\tau_{K+1}^{(0)}} + \tilde{c}_i \right) \right) (\tau_{K+1} - \tau_{K+1}^{(0)}) \\ & + \left(-\frac{1}{\sum_{j \neq i} \tilde{a}_{i,j} \frac{e_j^{(0)}}{\tau_{K+1}^{(0)}} + \tilde{c}_i} \right) \left(\sum_{j \neq i} \tilde{a}_{i,j} (e_j - e_j^{(0)}) \right), \end{aligned} \quad (25)$$

where $\tau_{K+1}^{(0)}$ and $e_j^{(0)}$ are feasible values for τ_{K+1} and e_j , respectively. Applying the SA method, the corresponding optimization problem in iteration l can be formulated as follows:

$$\begin{aligned} & \max_{\mathbf{e}, \tau, \{\tilde{\mathbf{W}}_i\}_{i=1}^K} R_{\text{new}}^{(l)} \\ & \text{s.t. (23.a) - (23.i)} \end{aligned} \quad (26)$$

where $R_{\text{new}}^{(l)}$ is given in (27) and superscript $(l-1)$ indicates the optimized value in iteration $(l-1)$.

$$\begin{aligned} R_{\text{new}}^{(l)} = & \sum_{i=1}^K \left(\tau_i \log \left(1 + \tilde{\beta}_i \frac{\text{Tr}(\tilde{\mathbf{F}}_i \tilde{\mathbf{W}}_i)}{\tau_i} \right) + \tau_{K+1} \log \left(1 + \sum_{j=1}^K \frac{\tilde{a}_{i,j}}{\tilde{c}_i} \frac{e_j}{\tau_{K+1}} \right) \right. \\ & \left. + \delta_{e,i}^{(l-1)} \left(\sum_{j \neq i} \tilde{a}_{i,j} e_j \right) + \delta_{\tau,i}^{(l-1)} \tau_{K+1} \right), \end{aligned} \quad (27)$$

$$\begin{aligned} \delta_{e,i}^{(l-1)} &= -\frac{1}{\frac{e_j^{(l-1)}}{\tau_{K+1}^{(l-1)}} + \tilde{c}_i}, \\ \delta_{\tau,i}^{(l-1)} &= \frac{\frac{e_j^{(l-1)}}{\tau_{K+1}^{(l-1)}}}{\frac{e_j^{(l-1)}}{\tau_{K+1}^{(l-1)}} + \tilde{c}_i} - \log \left(\sum_{j \neq i} \tilde{a}_{i,j} \frac{e_j^{(l-1)}}{\tau_{K+1}^{(l-1)}} + \tilde{c}_i \right) + \log(\tilde{c}_i). \end{aligned}$$

Now, the only source of non-convexity for problem (26) is the rank-one constraint in (23.i), which can be relaxed using the semidefinite relaxation (SDR) technique. The relaxed problem will be a convex optimization problem, which can be solved by convex optimization toolboxes (e.g., CVX). We iteratively maximize the lower bound of the total throughput by solving the relaxed version of (26) until a satisfactory convergence is achieved. As there is no guarantee for the optimized $\tilde{\mathbf{W}}_i$, denoted as $\tilde{\mathbf{W}}_i^{\text{opt}}$ to be rank-one, we use the eigen-decomposition technique to extract a feasible rank-one solution from it. Particularly, if $\tilde{\mathbf{W}}_i^{\text{opt}}$ is of rank r , we can express it as $\tilde{\mathbf{W}}_i^{\text{opt}} = \sum_{j=1}^r \lambda_{i,j} \hat{\mathbf{w}}_{i,j} \hat{\mathbf{w}}_{i,j}^H$, where $\lambda_{i,1} > \dots > \lambda_{i,r}$ are the eigenvalues of $\tilde{\mathbf{W}}_i^{\text{opt}}$ and $\hat{\mathbf{w}}_{i,1}, \dots, \hat{\mathbf{w}}_{i,r}$ are the corresponding eigenvectors. The rank-one approximation for $\tilde{\mathbf{W}}_i^{\text{opt}}$ can be then given by $\hat{\mathbf{W}}_i = \lambda_{i,1} \hat{\mathbf{w}}_{i,1} \hat{\mathbf{w}}_{i,1}^H$ and the optimized beamforming vector of the PS in the i -th time-slot ($i \in \mathcal{K}$) will be obtained as $\mathbf{w}_i^{\text{opt}} = \sqrt{\lambda_{i,1} / \tau_i^{\text{opt}}} \hat{\mathbf{w}}_{i,1}$. We finally have $p_i^{\text{opt}} = e_i^{\text{opt}} / \tau_{K+1}^{\text{opt}}, \forall i \in \mathcal{K}$.

Algorithm 3 summarizes the procedure for optimizing the network resource allocation and transmit beamforming vectors of the PS.

Algorithm 3: Optimization of Resource Allocation and Transmit Beamforming

$\Delta = 1, l = 0, R_{\text{new}}^{(0)} = 0;$
Initialize $\mathbf{e}^{(0)}$ and $\tau^{(0)};$
while $\Delta > \epsilon$ **do**
 $l = l + 1;$
 Update $\delta_{e,i}^{(l-1)}$ and $\delta_{\tau,i}^{(l-1)}, \forall i \in \mathcal{K};$
 Solve (26) using CVX;
 $\Delta = |R_{\text{new}}^{(l)} - R_{\text{new}}^{(l-1)}|;$
Use eigen-decomposition technique to obtain a feasible rank-one $\hat{\mathbf{W}}_i$ from $\tilde{\mathbf{W}}_i^{\text{opt}}, \forall i \in \mathcal{K};$
Set $e_i^{\text{opt}} = e_i^{(l)}, \forall i \in \mathcal{K}, \tau_i^{\text{opt}} = \tau_i^{(l)}, \forall i \in \mathcal{K}, \tau_{K+1}^{\text{opt}} = \tau_{K+1}^{(l)}, p_i^{\text{opt}} = \frac{e_i^{\text{opt}}}{\tau_{K+1}^{\text{opt}}}, \forall i \in \mathcal{K}, \mathbf{w}_i^{\text{opt}} = \sqrt{\lambda_{i,1} / \tau_i^{\text{opt}}} \hat{\mathbf{w}}_{i,1}, \forall i \in \mathcal{K};$

B. Design of IRS Reflection for Active IT and Receive Beamforming

Having fixed the receive beamforming at the AP, the problem for optimizing the IRS reflection during τ_{K+1} is

formulated as

$$\max_{\Theta_{K+1}} \sum_{i=1}^K \left(\log \left(1 + \frac{p_i |\mathbf{a}_i^H \mathbf{h}_i(\Theta_{K+1})|^2}{\sum_{j \neq i} p_j |\mathbf{a}_i^H \mathbf{h}_j(\Theta_{K+1})|^2 + \|\mathbf{a}_i^H\|^2 \sigma^2} \right) \right) \quad (28)$$

s.t. $0 \leq \alpha_{n,K+1} \leq 1, -\pi < \theta_{n,K+1} \leq \pi, \forall n \in \mathcal{N}. \quad (28.a)$

Problem (28) is not a convex optimization problem and finding its optimal solution is not straightforward. A sub-optimal solution may be obtained by using the techniques of SDR and SA as will be briefly discussed in the following.

Using the previously defined $\mathbf{V}_i, \forall i \in \mathcal{K}$ and setting $\mathbf{u}_{K+1} = [u_{1,K+1}, \dots, u_{N,K+1}]^T$ with $u_{n,K+1} = \alpha_{n,K+1} \exp(j\theta_{n,K+1})$, $\tilde{\mathbf{u}}_{K+1} = [\mathbf{u}_{K+1}^T \ 1]^T$, and $\tilde{\mathbf{U}}_{K+1} = \tilde{\mathbf{u}}_{K+1} \tilde{\mathbf{u}}_{K+1}^H$, and after dropping the rank-one constraint on $\tilde{\mathbf{U}}_{K+1}$, problem (28) is re-formulated as

$$\max_{\tilde{\mathbf{U}}_{K+1}} \sum_{i=1}^K \left(\log \left(1 + \frac{\text{Tr}(\mathbf{A}_{i,i} \tilde{\mathbf{U}}_{K+1})}{\text{Tr}(\tilde{\mathbf{A}}_i \tilde{\mathbf{U}}_{K+1}) + \|\mathbf{a}_i^H\|^2 \sigma^2} \right) \right) \quad (29)$$

$$\text{s.t. } [\tilde{\mathbf{U}}_{K+1}]_{n,n} \leq 1, \forall n \in \mathcal{N}, \quad (29.a)$$

$$[\tilde{\mathbf{U}}_{K+1}]_{N+1,N+1} = 1, \quad (29.b)$$

where

$$\mathbf{A}_{i,j} = p_j \begin{bmatrix} \mathbf{V}_j^H \mathbf{a}_i \mathbf{a}_i^H \mathbf{V}_j^H & \mathbf{V}_j^H \mathbf{a}_i \mathbf{a}_i^H \mathbf{c}_j \\ \mathbf{c}_j^H \mathbf{a}_i \mathbf{a}_i^H \mathbf{V}_j & 0 \end{bmatrix}, \forall i, j \in \mathcal{K},$$

and $\tilde{\mathbf{A}}_i = \sum_{j \neq i} \mathbf{A}_{i,j}$.

Clearly, problem (29) is still non-convex. Based on the product rule for logarithms, (29) is re-written as

$$\max_{\tilde{\mathbf{U}}_{K+1}} \sum_{i=1}^K \left(\log \left(\text{Tr}(\mathbf{A}_{i,i} \tilde{\mathbf{U}}_{K+1}) + \text{Tr}(\tilde{\mathbf{A}}_i \tilde{\mathbf{U}}_{K+1}) + \|\mathbf{a}_i^H\|^2 \sigma^2 \right) - \log \varsigma_i \right) \quad (30)$$

$$\text{s.t. } (29.a) \text{ and } (29.b),$$

$$\text{Tr}(\tilde{\mathbf{A}}_i \tilde{\mathbf{U}}_{K+1}) + \|\mathbf{a}_i^H\|^2 \sigma^2 \leq \varsigma_i, \forall i \in \mathcal{K}, \quad (30.a)$$

Problem (30) is still not convex because the objective function involves summation of concave and convex functions. This issue can be dealt with through the SA technique. Specifically, the convex term $-\log \varsigma_i$ can be approximated by its lower bound (i.e., first-order Taylor expansion). The resulting problem will be an SDP which can be iteratively solved via CVX, updating ς_i in each iteration until convergence is attained. Eventually, the rank-one extraction procedure must be performed to find a feasible rank-one solution for $\tilde{\mathbf{U}}_{K+1}$, from which a sub-optimal \mathbf{u}_{K+1} is obtained. A similar process as above can be applied for optimizing the receive beamformers at the AP ($\{\mathbf{a}_i\}_{i=1}^K$), fixing other optimization variables.

The above procedure for optimizing \mathbf{u}_{K+1} and $\{\mathbf{a}_i\}_{i=1}^K$ incurs considerable complexity as SDP problems must be solved several times for each sub-problem. This complexity increases with increasing the number of users, antennas at the AP, and IRS elements, and can be prohibitively high in large networks.

Herein, we propose an algorithm with lower complexity for optimizing the IRS reflection coefficients in time slot $K+1$, assuming MMSE receive beamforming at the AP. Specifically, using the relationship between mean square error

(MSE) and SINR in MMSE receivers, we can jointly optimize the MMSE receive beamforming vectors at the AP and the IRS reflection coefficients in the $(K+1)$ -th time slot, using the BCD technique.

Under the assumption of independence between different $s_{2,i}$'s and also between $s_{2,i}, \forall i \in \mathcal{K}$ and each element of the noise vector \mathbf{n} , the MSE for U_i 's information signal is given by

$$\begin{aligned} E_i &= \mathbb{E}[|\mathbf{a}_i^H \mathbf{y}_2 - s_{2,i}|^2] \\ &= \sum_{j=1}^K p_j |\mathbf{a}_i^H \mathbf{h}_j(\Theta_{K+1})|^2 - \sqrt{p_i} (\mathbf{a}_i^H \mathbf{h}_i(\Theta_{K+1}) + \mathbf{h}_i^H(\Theta_{K+1}) \mathbf{a}_i) \\ &\quad + \|\mathbf{a}_i^H\|^2 \sigma^2 + 1. \end{aligned} \quad (31)$$

The following theorem establishes an equivalence between throughput maximization and MSE minimization problems.

Theorem 1. *The problem in (28) is equivalent to the following problem*

$$\min_{\{\mathbf{a}_i\}_{i=1}^K, \omega, \Theta_{K+1}} \sum_{i=1}^K (\omega_i E_i - \log \omega_i) \quad (32)$$

s.t. (28.a),

where $\omega = [\omega_1, \dots, \omega_K]$, and ω_i is a weight variable associated with U_i .

Proof. Please refer to the Appendix. \square

Rewriting the MSE in (31) with respect to $\mathbf{V}_i, \forall i \in \mathcal{K}$ and \mathbf{u}_{K+1} , we have

$$\begin{aligned} E_i &= \mathbf{u}_{K+1}^H \left(\sum_{j=1}^K p_j \mathbf{V}_j^H \mathbf{a}_i \mathbf{a}_i^H \mathbf{V}_j \right) \mathbf{u}_{K+1} \\ &\quad + \mathbf{u}_{K+1}^H \left(\sum_{j=1}^K p_j \mathbf{V}_j^H \mathbf{a}_i \mathbf{a}_i^H \mathbf{c}_j - \sqrt{p_i} \mathbf{V}_i^H \mathbf{a}_i \right) \\ &\quad + \left(\sum_{j=1}^K p_j \mathbf{V}_j^H \mathbf{a}_i \mathbf{a}_i^H \mathbf{c}_j - \sqrt{p_i} \mathbf{V}_i^H \mathbf{a}_i \right)^H \mathbf{u}_{K+1} \\ &\quad + \sum_{j=1}^K p_j \mathbf{c}_j^H \mathbf{a}_i \mathbf{a}_i^H \mathbf{c}_j - \sqrt{p_i} (\mathbf{a}_i^H \mathbf{c}_i + \mathbf{c}_i^H \mathbf{a}_i) + \|\mathbf{a}_i^H\|^2 \sigma^2 + 1. \end{aligned} \quad (33)$$

According to Theorem 1, problem (28) can be re-formulated as

$$\min_{\{\mathbf{a}_i\}_{i=1}^K, \omega, \mathbf{u}_{K+1}} \sum_{i=1}^K (\omega_i E_i - \log \omega_i) \quad (34)$$

$$\text{s.t. } |u_{n,K+1}| \leq 1, \forall n \in \mathcal{N}, \quad (34.a)$$

Applying the BCD method, problem (34) can be alternately solved for $\{\mathbf{a}_i\}_{i=1}^K, \omega$ and \mathbf{u}_{K+1} in an iterative manner, where the optimum value for each variable is found in each iteration. Particularly, denoting $\mathbf{u}_{K+1}^{(l-1)}$ as the optimal value for \mathbf{u}_{K+1} in

the $(l-1)$ -th iteration, the optimal receive beamforming vector for U_i in iteration l is given by

$$\mathbf{a}_i^{(l)} = \sqrt{p_i} \left(\sum_{j=1}^K p_j \left((\mathbf{V}_j \mathbf{u}_{K+1}^{(l-1)} + \mathbf{c}_j)(\mathbf{V}_j \mathbf{u}_{K+1}^{(l-1)} + \mathbf{c}_j)^H \right) + \sigma^2 \mathbf{I}_{M_A} \right)^{-1} \times (\mathbf{V}_i \mathbf{u}_{K+1}^{(l-1)} + \mathbf{c}_i), \quad \forall i \in \mathcal{K}, \quad (35)$$

and the optimal value for ω_i in the l -th iteration is given by

$$\omega_i^{(l)} = \frac{1}{E_i^{(l)}}, \quad \forall i \in \mathcal{K}, \quad (36)$$

where $E_i^{(l)}$ is obtained by substituting $\mathbf{u}_{K+1}^{(l-1)}$ and $\mathbf{a}_i^{(l)}$ into (33). Finally, with $\{\mathbf{a}_i^{(l)}\}_{i=1}^K$ and $\omega^{(l)}$, the problem for optimizing \mathbf{u}_{K+1} in the l -th iteration is formulated as

$$\min_{\mathbf{u}_{K+1}} \mathbf{u}_{K+1}^H \mathbf{B}^{(l)} \mathbf{u}_{K+1} - 2\text{Re}\{\mathbf{b}^{(l)H} \mathbf{u}_{K+1}\} \quad (37)$$

$$\text{s.t. } \mathbf{u}_{K+1}^H \mathbf{D}_n \mathbf{u}_{K+1} \leq 1, \quad \forall n \in \mathcal{N}, \quad (37.a)$$

where

$$\mathbf{B}^{(l)} = \sum_{i=1}^K \omega_i \sum_{j=1}^K p_j \mathbf{V}_j^H \mathbf{a}_i^{(l)} \mathbf{a}_i^{(l)H} \mathbf{V}_j$$

$$\mathbf{b}^{(l)} = \sum_{i=1}^K \omega_i \left(\sqrt{p_i} \mathbf{V}_i^H \mathbf{a}_i^{(l)} - \sum_{j=1}^K p_j \mathbf{V}_j^H \mathbf{a}_i^{(l)} \mathbf{a}_i^{(l)H} \mathbf{c}_j \right),$$

and \mathbf{D}_n is a diagonal matrix with 1 on its n -th diagonal element and 0 elsewhere. (37) is a convex quadratically-constrained quadratic program (QCQP) and can be solved using convex optimization techniques. We use the Lagrange duality method to solve (37) for which the Lagrangian is given by

$$\mathcal{L} = \mathbf{u}_{K+1}^H \mathbf{B}^{(l)} \mathbf{u}_{K+1} - 2\text{Re}\{\mathbf{b}^{(l)H} \mathbf{u}_{K+1}\} + \sum_{n=1}^N \mu_n (\mathbf{u}_{K+1}^H \mathbf{D}_n \mathbf{u}_{K+1} - 1), \quad (38)$$

with $\boldsymbol{\mu} = [\mu_1, \dots, \mu_N]$ being the Lagrange multipliers associated with the constraint (37.a). The first-order optimality condition of \mathcal{L} with respect to \mathbf{u}_{K+1} yields

$$\mathbf{u}_{K+1}(\boldsymbol{\mu}) = (\mathbf{B}^{(l)} + \sum_{n=1}^N \mu_n \mathbf{D}_n)^{-1} \mathbf{b}^{(l)}. \quad (39)$$

$\boldsymbol{\mu}$ can be updated via the ellipsoid method with the subgradient of μ_n being given by $|\mathbf{u}_{n,K+1}|^2 - 1$.

Algorithm 4 describes the steps for optimizing the IRS reflection coefficients for assisting users' active information transfer, when MMSE receiver is used at the AP. By alternately running algorithms 3 and 4 until convergence, the near-optimal resource allocation, transmit and receive beamforming, and IRS reflection for active IT are obtained.

Remark 2. Matrix $\mathbf{B}^{(l)}$ is the summation of K^2 rank-one matrices. If $K^2 \geq N$, matrix $\mathbf{B}^{(l)}$ is full-rank and invertible and so is $\mathbf{B}^{(l)} + \sum_{n=1}^N \mu_n \mathbf{D}_n$. If $K^2 < N$, the invertibility of

Algorithm 4: Optimization of IRS Reflection for Active IT and Receive Beamforming

```

Set  $\mathbf{u}_{n,K+1}^{(0)} = 1, \forall n \in \mathcal{N}$ ;
 $\Delta = 1, l = 0$ ;
Initialize  $\omega^{(0)}$ ;
while  $\Delta > \epsilon$  do
     $l = l + 1$ ;
    Obtain  $\mathbf{a}_i^{(l)}, \forall i \in \mathcal{K}$  from (35);
    Obtain  $\omega_i^{(l)}, \forall i \in \mathcal{K}$  from (36);
    Obtain  $\mathbf{u}_{K+1}^{(l)}$  by solving the QCQP in (37);
     $\Delta = |\sum_{i=1}^K \log(\omega_i^{(l)}) - \sum_{i=1}^K \log(\omega_i^{(l-1)})|$ ;
Set  $\alpha_{n,K+1}^* = |\mathbf{u}_{n,K+1}^{(l)}|, \theta_{n,K+1}^* = \arg(\mathbf{u}_{n,K+1}^{(l)}), \forall n \in \mathcal{N}$  and
 $\mathbf{a}_i^* = \mathbf{a}_i^{(l)}, \forall i \in \mathcal{K}$ ;

```

$\mathbf{B}^{(l)} + \sum_{n=1}^N \mu_n \mathbf{D}_n$ depends on the value of μ_n 's and is not guaranteed; but problem (37) is still a QCQP and can be solved using CVX solvers.

V. PERFORMANCE EVALUATION

The objective of this section is to evaluate the performance of the proposed IRS-empowered system and demonstrate the gain brought by the integration of IRS into BS-WPCNs. Along with the results reported in our previous work [18] which showed the benefits of integrating backscatter communication and wireless powered communication, the results of this section substantiates the promising benefits of integrating these three important technologies, i.e., wireless powered communication, backscatter communication, and intelligent reflecting surface.

A. Simulation Setup

We consider a 2-D Cartesian coordinate system, as shown in Fig. 4, where the AP is located at the origin, the reference element of the IRS is placed at $(x_{\text{IRS}}, y_{\text{IRS}})$ and the PS is positioned at $(x_{\text{PS}}, 0)$. K users are evenly placed on the left half-circle centered at the PS with radius r . Parameters η, ξ , and p_{sat} for the EH model at the users are obtained by fitting the model in (1) to the real measurements reported in [40]. All channels are modeled by the Rician fading channel model [22], [24], [25], [29]. For example, the channel between the AP and the IRS is given by

$$\mathbf{H} = \sqrt{\frac{\kappa_h}{\kappa_h + 1}} \mathbf{H}^{\text{LoS}} + \sqrt{\frac{1}{\kappa_h + 1}} \mathbf{H}^{\text{NLoS}}, \quad (40)$$

where κ_h is the Rician factor, and $\mathbf{H}^{\text{LoS}} \in \mathbb{C}^{M_A \times N}$ and $\mathbf{H}^{\text{NLoS}} \in \mathbb{C}^{M_A \times N}$ are the line-of-sight (LoS) and non-line-of-sight (NLoS) components of \mathbf{H} . The LoS channel matrix is modeled as $\mathbf{H}^{\text{LoS}} = \hat{\mathbf{h}}_{M_A}(\varphi_{\text{AoA}}) \hat{\mathbf{h}}_N^H(\varphi_{\text{AoD}})$, where φ_{AoA} and φ_{AoD} denote the angle of arrival and angle of departure of IRS, respectively, and $\hat{\mathbf{h}}_X(\varphi) = [1, e^{j\pi \sin(\varphi)}, e^{j2\pi \sin(\varphi)}, \dots, e^{j(X-1)\pi \sin(\varphi)}]^T$. The elements in \mathbf{H} are then multiplied by the square root of the distance-dependent path-loss $C_0(d_h/D_0)^{-\rho_h}$, where C_0 is the path-loss at the reference distance of $D_0 = 1$ meter (m), set as $C_0 = -30$ dBm, d_h represents the distance between AP and IRS, and ρ_h is the path-loss exponent of the channel between the AP and

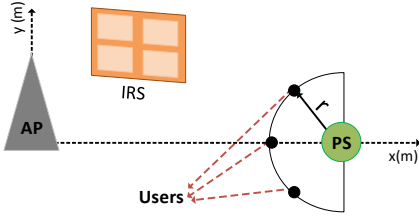


Fig. 4: Simulation setup

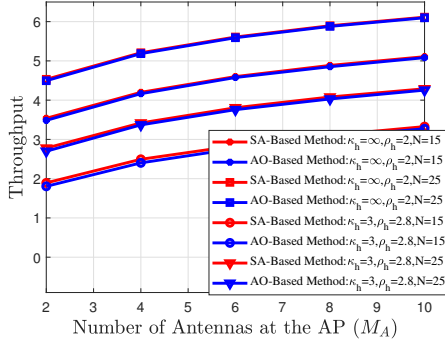


Fig. 5: Comparison between SA-based and AO-based methods

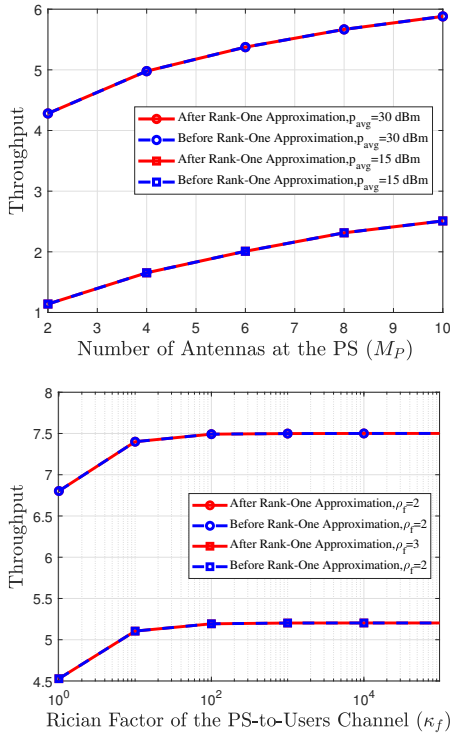


Fig. 6: Throughput with and without rank-one approximation

the IRS. Channels F , G , and C are defined in a similar way as H , with κ_f , κ_g , and κ_c being the corresponding Rician factors, and ρ_f , ρ_g , and ρ_c denoting the path-loss exponents of the corresponding channels.

Unless otherwise stated, the following set of parameters are used: The number of users K is assumed to be 10. The number of antennas at the PS and the AP is set as 5, i.e., $M_P = M_A = 5$, and the number of elements at the IRS is set to be 25, i.e., $N = 25$. The following coordinates are used for the IRS and

the PS: $x_{\text{IRS}} = y_{\text{IRS}} = 5$ m, $x_{\text{PS}} = 35$ m. Also, the distance from the users to the PS is set as $r = 10$ m. The channel-related parameters used in simulations are $\kappa_h = \infty$, $\kappa_f = \kappa_g = 3$, $\kappa_c = 0$, $\rho_h = 2$, $\rho_f = \rho_g = 2.8$, $\rho_c = 3.5$. EH model parameters are obtained as $\eta = 0.47$, $\xi = 2.24 \times 10^{-5}$, and $p_{\text{sat}} = 45$ mW. Maximum average power at the PS is set as $p_{\text{avg}} = 1$ W and for the peak power at the PS we use $p_{\text{peak}} = 2p_{\text{avg}}$. Backscatter coefficient is set as $\beta_i = 0.6$, $\forall i \in \mathcal{K}$ and the circuit power consumption for active IT is assumed to be $p_{c,i} = 10$ mW, $\forall i \in \mathcal{K}$. The noise power spectral density is -160 dBm/Hz and the bandwidth is 1 MHz. The unit for the sum-throughput is thus Mnats/s. The stopping threshold for convergence is set as $\epsilon = 0.001$ in all algorithms. The AP is assumed to apply MMSE receive beamforming for detecting users' active information signals. The results are based on the average of 1000 different channel realizations.

B. Numerical Results

Fig. 5 compares the performance of the SA-based and AO-based methods for optimizing the reflection coefficients of the IRS elements when assisting in the users' backscatter transmission to the AP. The figure shows the network throughput versus the number of AP antennas for different IRS-AP channel conditions and number of IRS elements. It can be seen that the SA-based method performs slightly better than the AO-based method; that's because in the SA-based method, the reflection coefficients of the IRS are jointly optimized in each iteration, while AO-based method optimizes each reflection coefficient individually. Due to the superiority of the SA-based method, we use this method in subsequent simulations.

Next, we show the tightness of the rank-one approximation in Algorithm 3. To this end, we compare the throughput of the proposed scheme to the calculated throughput when no rank-one approximation is performed. Fig. 6 compares the maximized throughput before and after rank-one approximation. The solid red lines represent the throughput performance of our proposed scheme when Eigen-decomposition is performed in Algorithm 3 for obtaining the beamforming vectors at the PS, while for the dotted blue lines, the throughput is calculated based on $\tilde{\mathbf{W}}_i^{\text{opt}}$, $\forall i \in \mathcal{K}$ without extracting the beamforming vectors $\mathbf{w}_i^{\text{opt}}$, $\forall i \in \mathcal{K}$. The close match between the calculated throughputs with and without rank-one approximation validates the accuracy of the Eigen-decomposition-based technique for extracting feasible rank-one matrices $\tilde{\mathbf{W}}_i$ from $\tilde{\mathbf{W}}_i^{\text{opt}}$, $\forall i \in \mathcal{K}$.

Fig. 7–Fig. 11 study the performance of our proposed IRS-empowered BS-WPCN by comparing it to two benchmarks, labeled as "Random Phase Shifts" and "Without IRS" on the figures. In particular, the former corresponds to a scheme in which the IRS reflection coefficients are randomly chosen in all $K + 1$ time slots, while other variables are optimized based on the techniques discussed throughout the paper. The latter benchmark represents a BS-WPCN network with no IRS, where the users can communicate with the AP only via the direct link. Furthermore, the dotted red lines refer to the proposed scheme after applying a 2-bit-resolution phase quantization to the optimized phase shifts of IRS elements

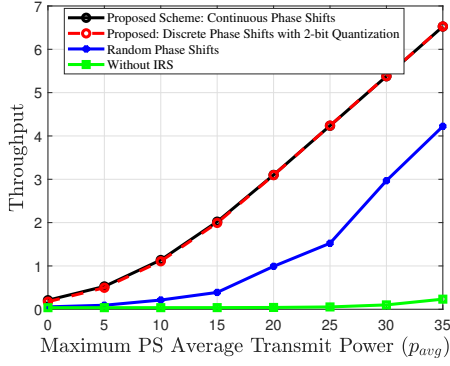


Fig. 7: Throughput vs. average transmit power of the PS

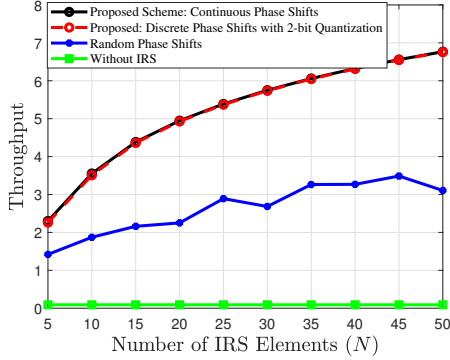


Fig. 8: Throughput vs. number of IRS elements

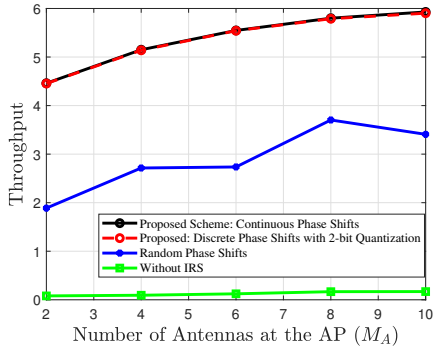


Fig. 9: Throughput vs. number of antennas at the AP

in each time slot. Particularly, each optimized continuous phase shift is quantized to its closest value from the set $\{-\frac{3\pi}{4}, -\frac{\pi}{4}, \frac{\pi}{4}, \frac{3\pi}{4}\}$, and the throughput is calculated based on the quantized phase shifts.

As expected, the throughput improves with increasing the maximum average PS transmit power, number of IRS reflecting elements, and number of antennas at the AP and PS (Fig. 7–Fig. 10). When increasing the distance between the PS and users (Fig. 11), the throughput first decreases because the received power from the PS is reduced, so is the power of the users' transmitted signals in both backscatter and active IT. However, the throughput begins to increase after some point because the users get closer to the IRS and the AP, meaning that the signals transmitted by the users get less attenuated before reaching the IRS and the AP.

It is well observed that our proposed method performs remarkably better than the benchmark schemes, which endorses

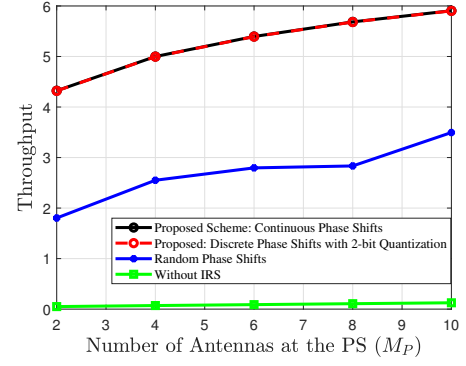


Fig. 10: Throughput vs. number of antennas at the PS

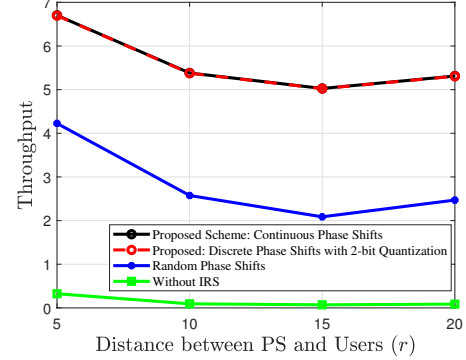


Fig. 11: Throughput vs. PS-to-users distance

the advantage of using IRS for assisting the communication between the users and the AP in the BS-WPCN. It can also be seen that the scheme with random selection of IRS phase shifts undergoes fluctuations, which is due to the fact that the randomly-chosen phase shifts may not result in coherent combination of the reflected signals from different user-IRS-AP paths. However, even with random IRS phase shifts, the IRS-assisted network significantly outperforms the scheme without IRS. This again confirms that employing IRS is a promising approach for improving the performance of existing communication networks.

Another important observation is that the performance gap between the scheme with continuous phase shifts and the one with quantized phase shifts is very negligible, which indicates that our proposed algorithms can be applied to practical IRS-assisted systems with discrete phase shift values for the IRS elements.

VI. CONCLUDING REMARKS AND FUTURE OUTLOOK

This paper studied a multi-user BS-WPCN, where the backscatter and active IT of the users to the AP are assisted by an IRS. We investigated the optimal design of IRS reflection coefficients, power allocation for the users' active IT, transmit beamforming of the PS, receive beamforming of the AP, and time allocation, for maximizing the total throughput of the network. A two-stage scheme has been proposed, with IRS reflection coefficients for assisting the backscatter transmission of the users being optimized in the first stage, while dealing with the optimization of other variables in the second stage. We presented two methods based on AO and SA techniques

for the first-stage optimization. In the second stage, we have used the SDR and SA techniques for optimizing AP transmit beamforming vectors, power and time allocation. Also, assuming an MMSE receiver at the AP, an efficient algorithm based on the BCD technique has been presented for jointly optimizing the AP receive beamforming vectors and IRS reflection coefficients when assisting the users' active IT. The accuracy and effectiveness of the proposed algorithms have been validated via numerical simulations.

This paper can be extended by taking the energy budget of IRS elements into account. Another possible extension is to use two or more IRSs which can cooperatively assist the transmission of users to the AP. All in all, although IRS has lately attracted substantial research efforts, there are still gaps to be filled. Specifically, the theoretical results on IRS need to be upheld via testbed experiments, to attest the effectiveness of integrating IRS into existing wireless networks.

APPENDIX: PROOF OF THEOREM 1

Fixing ω and Θ_{K+1} , (32) is convex with respect to \mathbf{a}_i , $\forall i \in \mathcal{K}$, the optimal value of which can be obtained from the first-order optimality condition as

$$\mathbf{a}_i^* = \sqrt{p_i} \left(\sum_{j=1}^K p_j \mathbf{h}_j(\Theta_{K+1}) \mathbf{h}_j^H(\Theta_{K+1}) + \sigma^2 \mathbf{I}_{M_A} \right)^{-1} \mathbf{h}_i(\Theta_{K+1}), \quad (41)$$

where the receive beamforming vector in (41) is the well-known MMSE receiver which minimizes the MSE as

$$E_{i,\min} = 1 - p_i \mathbf{h}_i^H(\Theta_{K+1}) J^{-1} \mathbf{h}_i(\Theta_{K+1}), \quad (42)$$

with $J = \sum_{j=1}^K p_j \mathbf{h}_j(\Theta_{K+1}) \mathbf{h}_j^H(\Theta_{K+1}) + \sigma^2 \mathbf{I}_{M_A}$.

Having $\{\mathbf{a}_i^*\}_{i=1}^K$ and Θ_{K+1} fixed, the weight ω_i for minimizing (32) is obtained as

$$\omega_i^* = E_{i,\min}^{-1}. \quad (43)$$

Now, the problem for optimizing Θ_{K+1} is obtained by substituting (41) and (43) into (32) as

$$\begin{aligned} \min_{\Theta_{K+1}} \quad & - \sum_{i=1}^K \log(E_{i,\min}^{-1}) = \max_{\Theta_{K+1}} \sum_{i=1}^K \log(E_{i,\min}^{-1}) \\ \text{s.t.} \quad & (28.a), \end{aligned} \quad (44)$$

We drop the argument Θ_{K+1} in the sequel for simplicity of

notation. We have

$$\begin{aligned} E_{i,\min}^{-1} &= (1 - p_i \mathbf{h}_i^H J^{-1} \mathbf{h}_i)^{-1} = \left(\frac{p_i \mathbf{h}_i^H J^{-1} \mathbf{h}_i - (p_i \mathbf{h}_i^H J^{-1} \mathbf{h}_i)^2}{p_i \mathbf{h}_i^H J^{-1} \mathbf{h}_i} \right)^{-1} \\ &= \frac{p_i \mathbf{h}_i^H J^{-1} \mathbf{h}_i}{p_i \mathbf{h}_i^H J^{-1} \mathbf{h}_i - (p_i \mathbf{h}_i^H J^{-1} \mathbf{h}_i)^2} = 1 + \frac{(p_i \mathbf{h}_i^H J^{-1} \mathbf{h}_i)^2}{p_i \mathbf{h}_i^H J^{-1} \mathbf{h}_i - (p_i \mathbf{h}_i^H J^{-1} \mathbf{h}_i)^2} \\ &\stackrel{(\varpi_4)}{=} 1 + \frac{(p_i \mathbf{h}_i^H J^{-1} \mathbf{h}_i)^2}{p_i \mathbf{h}_i^H J^{-1} J J^{-1} \mathbf{h}_i - (p_i \mathbf{h}_i^H J^{-1} \mathbf{h}_i)^2} \\ &= 1 + \frac{(p_i \mathbf{h}_i^H J^{-1} \mathbf{h}_i)^2}{p_i \mathbf{h}_i^H J^{-1} (J - p_i \mathbf{h}_i \mathbf{h}_i^H) J^{-1} \mathbf{h}_i} \\ &= 1 + \frac{(p_i \mathbf{h}_i^H J^{-1} \mathbf{h}_i)^2}{p_i \mathbf{h}_i^H J^{-1} (\sum_{j \neq i} p_j \mathbf{h}_j \mathbf{h}_j^H + \sigma^2 \mathbf{I}_{M_A}) J^{-1} \mathbf{h}_i} \\ &\stackrel{(\varpi_5)}{=} 1 + \frac{p_i |\mathbf{a}_i^*{}^H \mathbf{h}_i(\Theta_{K+1})|^2}{\sum_{j \neq i} p_j |\mathbf{a}_i^*{}^H \mathbf{h}_j(\Theta_{K+1})|^2 + \|\mathbf{a}_i^*{}^H\|^2 \sigma^2} = 1 + \gamma_{2,i,\text{mmse}}, \end{aligned} \quad (45)$$

where $\gamma_{2,i,\text{mmse}}$ is the SINR of U_i for active IT, when MMSE receive beamforming is employed at the AP. In (45), (ϖ_4) holds because $p_i \mathbf{h}_i^H J^{-1} J J^{-1} \mathbf{h}_i = p_i \mathbf{h}_i^H J^{-1} \mathbf{h}_i$ and (ϖ_5) holds because $\mathbf{a}_i^* = \sqrt{p_i} J^{-1} \mathbf{h}_i$. The proof is completed by substituting (45) into (44).

REFERENCES

- [1] S. Bi, C. K. Ho, and R. Zhang, "Wireless Powered Communication: Opportunities and Challenges," in *IEEE Commun. Mag.*, vol. 53, no. 4, pp. 117-125, Apr. 2015.
- [2] S. Bi, Y. Zeng, and R. Zhang, "Wireless Powered Communication Networks: An Overview," in *IEEE Wireless Commun.*, vol. 23, no. 2, pp. 10-18, Apr. 2016.
- [3] D. Niyato, D. I. Kim, M. Maso, and Z. Han, "Wireless Powered Communication Networks: Research Directions and Technological Approaches," in *IEEE Wireless Commun.*, vol. 24, no. 6, pp. 88-97, Dec. 2017.
- [4] H. Ju and R. Zhang, "Throughput Maximization in Wireless Powered Communication Networks," in *IEEE Trans. Wireless Commun.*, vol. 13, no. 1, pp. 418-428, Jan. 2014.
- [5] Q. Sun, G. Zhu, C. Shen, X. Li, and Z. Zhong, "Joint Beamforming Design and Time Allocation for Wireless Powered Communication Networks," in *IEEE Commun. Lett.*, vol. 18, no. 10, pp. 1783-1786, Oct. 2014.
- [6] L. Liu, R. Zhang, and K-C. Chua, "Multi-Antenna Wireless Powered Communication With Energy Beamforming," in *IEEE Trans. Commun.*, vol. 62, no. 12, pp. 4349-4361, Dec. 2014.
- [7] H. Ju and R. Zhang, "Optimal Resource Allocation in Full-Duplex Wireless-Powered Communication Network," in *IEEE Trans. Commun.*, vol. 62, no. 10, pp. 3528-3540, Oct. 2014.
- [8] Y. Zeng and R. Zhang, "Optimized Training Design for Wireless Energy Transfer," in *IEEE Trans. Wireless Commun.*, vol. 63, no. 2, pp. 536-550, Feb. 2015.
- [9] H. Ju and R. Zhang, "User Cooperation in Wireless Powered Communication Networks," in *Proc. IEEE GLOBECOM*, Austin, TX, USA, Dec. 2014, pp. 1430-1435.
- [10] H. Chen, Y. Li, J. L. Rebelatto, B. F. Uchôa-Filho, and B. Vucetic, "Harvest-Then-Cooperate: Wireless-Powered Cooperative Communications," in *IEEE Trans. Signal Process.*, vol. 63, no. 7, pp. 1700-1711, Apr. 2015.
- [11] X. Di, K. Xiong, P. Fan, H-C. Yang, and K. H. Letaief, "Optimal Resource Allocation in Wireless Powered Communication Networks With User Cooperation," in *IEEE Trans. Wireless Commun.*, vol. 16, no. 12, pp. 7936-7949, Dec. 2017.
- [12] Y. Ma, H. Chen, Z. Lin, Y. Li, and B. Vucetic, "Distributed and Optimal Resource Allocation for Power Beacon-Assisted Wireless-Powered Communications," in *IEEE Trans. Commun.*, vol. 63, no. 10, pp. 3569-3583, Oct. 2015.
- [13] S. Lohani, R. A. Loodaricheh, E. Hossain, and V. K. Bhargava, "On Multiuser Resource Allocation in Relay-Based Wireless-Powered Uplink Cellular Networks," in *IEEE Trans. Wireless Commun.*, vol. 15, no. 3, pp. 1851-1865, Mar. 2016.

- [14] P. Ramezani, Y. Zeng, and A. Jamalipour, "Optimal Resource Allocation for Multiuser Internet of Things Network With Single Wireless-Powered Relay," in *IEEE Internet of Things J.*, vol. 6, no. 2, pp. 3132-3142, Apr. 2019.
- [15] J. Xu *et al.*, "Robust Transmissions in Wireless-Powered Multi-Relay Networks With Chance Interference Constraints," in *IEEE Trans. Commun.*, vol. 67, no. 2, pp. 973-987, Feb. 2019.
- [16] P. Ramezani and A. Jamalipour, "Two-Way Dual-Hop WPCN With A Practical Energy Harvesting Model," in *IEEE Trans. Veh. Technol.*, vol. 69, no. 7, pp. 8013-8017, Jul. 2020.
- [17] S. H. Kim and D. I. Kim, "Hybrid Backscatter Communication for Wireless-Powered Heterogeneous Networks," in *IEEE Trans. Wireless Commun.*, vol. 16, no. 10, pp. 6557-6570, Oct. 2017.
- [18] P. Ramezani and A. Jamalipour, "Optimal Resource Allocation in Backscatter Assisted WPCN With Practical Energy Harvesting Model," in *IEEE Trans. Veh. Technol.*, vol. 68, no. 12, pp. 12406-12410, Dec. 2019.
- [19] X. Lu, D. Niyato, D. I. Kim, Y. Xiao, and Z. Han "Ambient Backscatter Assisted Wireless Powered Communications," in *IEEE Wireless Commun.*, vol. 25, no. 2, pp. 170-177, Apr. 2018.
- [20] N. V. Huynh *et al.*, "Ambient Backscatter Communications: A Contemporary Survey," in *IEEE Commun. Surveys Tuts.*, vol. 20, no. 4, pp. 2889-2922, 4th Quart. 2018.
- [21] X. Yu, D. Xu, and R. Schober, "MISO Wireless Communication Systems via Intelligent Reflecting Surfaces," in *Proc. IEEE/CIC ICC*, Changchun, China, Aug. 2019, pp. 735-740.
- [22] D. Mishra and H. Johansson, "Channel Estimation and Low-complexity Beamforming Design for Passive Intelligent Surface Assisted MISO Wireless Energy Transfer," in *Proc. IEEE ICASSP*, Brighton, U.K., May 2019, pp. 1-5.
- [23] Z.-Q. He and X. Yuan, "Cascaded Channel Estimation for Large Intelligent Metasurface Assisted Massive MIMO," in *IEEE Wireless Commun. Lett.*, vol. 9, no. 2, pp. 210-214, Feb. 2020.
- [24] S. Zhang and R. Zhang, "Capacity Characterization for Intelligent Reflecting Surface Aided MIMO Communication," in *IEEE J. Sel. Areas Commun.*, vol. 38, no. 8, pp. 1823-1838, Aug. 2020.
- [25] W. Yan, X. Yuan, Z.-Q. He, and X. Kuai, "Passive Beamforming and Information Transfer Design for Reconfigurable Intelligent Surfaces Aided Multiuser MIMO Systems," in *IEEE J. Sel. Areas Commun.*, vol. 38, no. 8, pp. 1793-1808, Aug. 2020.
- [26] Z. Abdullah, G. Chen, S. Lambbotharan, and J. A. Chambers, "Optimization of Intelligent Reflecting Surface Assisted Full-Duplex Relay Networks," in *IEEE Wireless Commun. Lett.*, vol. 10, no. 2, pp. 363-367, Feb. 2021.
- [27] Q. Wu and R. Zhang, "Weighted Sum Power Maximization for Intelligent Reflecting Surface Aided SWIPT," in *IEEE Wireless Commun. Lett.*, vol. 9, no. 5, pp. 586-590, May 2020.
- [28] Y. Zheng, S. Bi, Y. J. Zhang, and H. Wang, "Intelligent Reflecting Surface Enhanced User Cooperation in Wireless Powered Communication Networks," in *IEEE Wireless Commun. Lett.*, vol. 9, no. 6, pp. 901-905, Jun. 2020.
- [29] B. Lyu *et al.*, "Optimized Energy and Information Relaying in Self-Sustainable IRS-Empowered WPCN," in *IEEE Trans. Commun.*, vol. 69, no. 1, pp. 619-633, Jan. 2021.
- [30] Q. Wu and R. Zhang, "Towards Smart and Reconfigurable Environment: Intelligent Reflecting Surface Aided Wireless Network," in *IEEE Commun. Mag.*, vol. 58, no. 1, pp. 106-112, Jan. 2020.
- [31] S. Gong *et al.*, "Toward Smart Wireless Communications via Intelligent Reflecting Surfaces: A Contemporary Survey," in *IEEE Commun. Surveys Tuts.*, vol. 22, no. 4, pp. 2283-2314, 4th Quart. 2020.
- [32] Q. Wu, S. Zhang, B. Zheng, C. You, and R. Zhang, "Intelligent Reflecting Surface Aided Wireless Communications: A Tutorial," in *IEEE Trans. Commun.*, Early Access, 2021.
- [33] J. Guo and X. Zhu, "An Improved Analytical Model for RF-DC Conversion Efficiency in Microwave Rectifiers," in *IEEE MTT-S Int. Microw. Symp. Dig.*, Jun. 2012, pp. 1-3.
- [34] C. R. Valenta and G. D. Durgin, "Harvesting Wireless Power: Survey of Energy-Harvester Conversion Efficiency in Far-Field, Wireless Power Transfer Systems," in *IEEE Microw. Mag.*, vol. 15, no. 4, pp. 108-120, Jun. 2014.
- [35] E. Boshkovska, D. W. K. Ng, L. Dai, and R. Schober, "Power-Efficient and Secure WPCNs With Hardware Impairments and Non-Linear EH Circuit," in *IEEE Trans. Commun.*, vol. 66, no. 6, pp. 2642-2657, Jun. 2018.
- [36] B. Clerckx *et al.*, "Fundamentals of Wireless Information and Power Transfer: From RF Energy Harvester Models to Signal and System Designs," in *IEEE J. Sel. Areas Commun.*, vol. 37, no. 1, pp. 4-33, Jan. 2019.
- [37] M. Grant and S. Boyd, "CVX: MATLAB Software for Disciplined Convex Programming", Version 2.2 [Online], Available: <http://cvxr.com/cvx>, Jan. 2020.
- [38] G. Papotto, F. Carrara, and G. Palmisano, "A 90-nm CMOS Threshold-Compensated RF Energy Harvester," in *IEEE J. Solid-State Circuits*, vol. 46, no. 9, pp. 1985-1997, Sep. 2011.
- [39] M. Stoopman, S. Keyrouz, H. J. Visser, K. Philips, and W. A. Serdijn, "Co-Design of a CMOS Rectifier and Small Loop Antenna for Highly Sensitive RF Energy Harvesters," in *IEEE J. Solid-State Circuits*, vol. 49, no. 3, pp. 622-634, Mar. 2014.
- [40] D. Khan *et al.*, "A CMOS RF Energy Harvester With 47% Peak Efficiency Using Internal Threshold Voltage Compensation," in *IEEE Microw. Wireless Compon. Lett.*, vol. 29, no. 6, pp. 415-417, Jun. 2019.